

Article

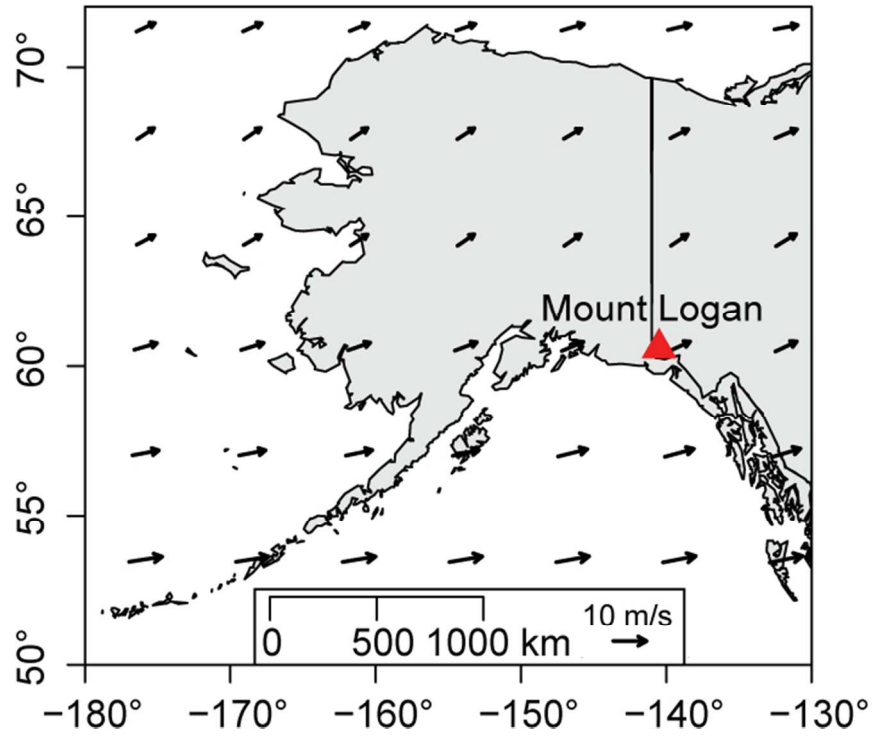
An ice core perspective on mercury pollution during the past 600 years

Samuel Beal, Erich C. Osterberg, Chris Zdanowicz, and David Fisher

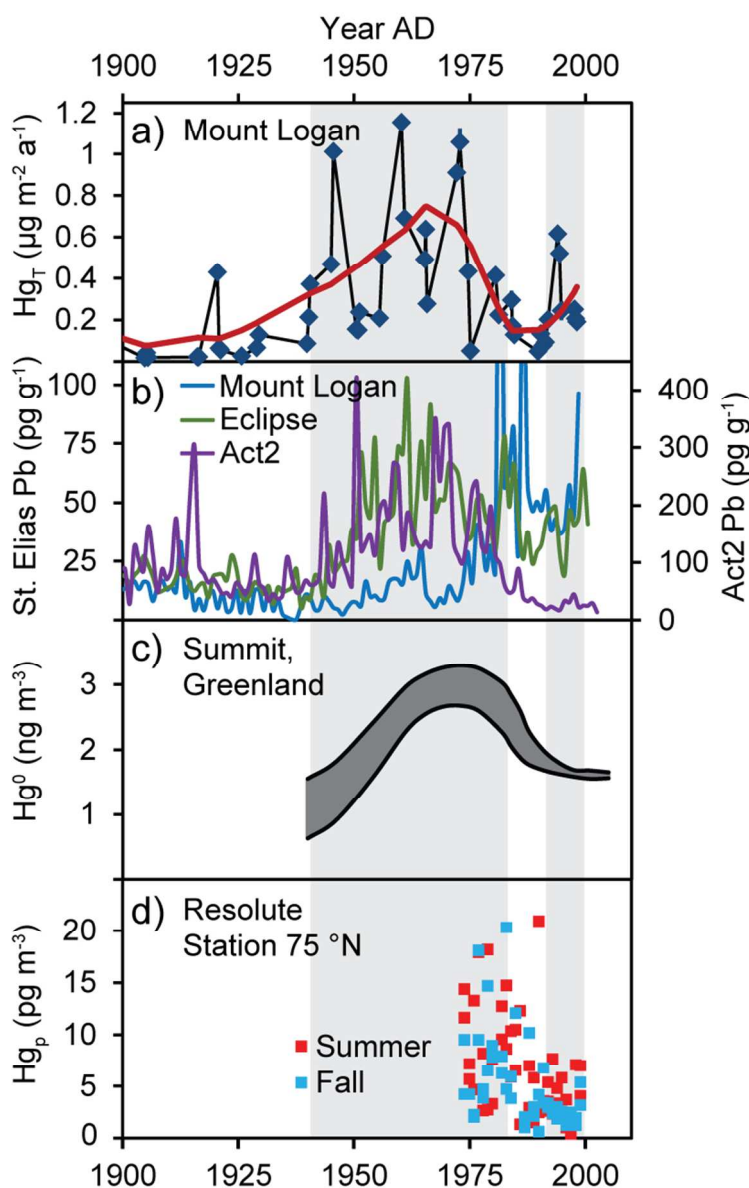
Environ. Sci. Technol., **Just Accepted Manuscript** • DOI: 10.1021/acs.est.5b01033 • Publication Date (Web): 26 May 2015Downloaded from <http://pubs.acs.org> on May 31, 2015

Just Accepted

“Just Accepted” manuscripts have been peer-reviewed and accepted for publication. They are posted online prior to technical editing, formatting for publication and author proofing. The American Chemical Society provides “Just Accepted” as a free service to the research community to expedite the dissemination of scientific material as soon as possible after acceptance. “Just Accepted” manuscripts appear in full in PDF format accompanied by an HTML abstract. “Just Accepted” manuscripts have been fully peer reviewed, but should not be considered the official version of record. They are accessible to all readers and citable by the Digital Object Identifier (DOI®). “Just Accepted” is an optional service offered to authors. Therefore, the “Just Accepted” Web site may not include all articles that will be published in the journal. After a manuscript is technically edited and formatted, it will be removed from the “Just Accepted” Web site and published as an ASAP article. Note that technical editing may introduce minor changes to the manuscript text and/or graphics which could affect content, and all legal disclaimers and ethical guidelines that apply to the journal pertain. ACS cannot be held responsible for errors or consequences arising from the use of information contained in these “Just Accepted” manuscripts.

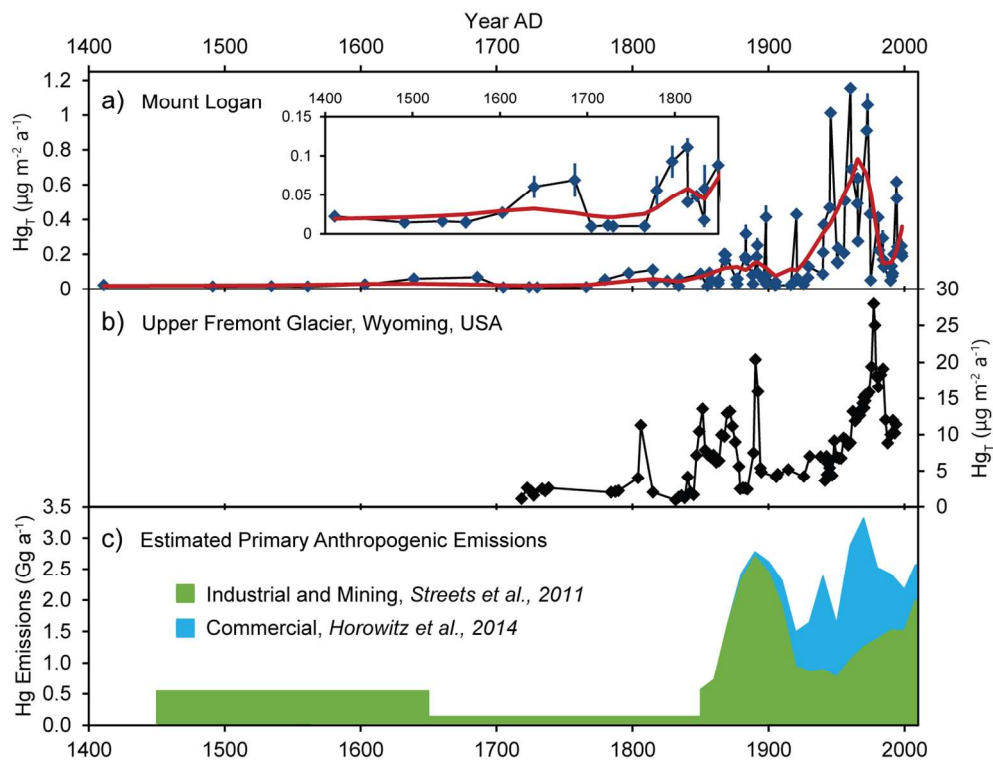


Location of Mount Logan (red triangle) in the St. Elias Mountains on the border of Alaska and Yukon, Canada. Arrows represent annual average vector wind at 500 mb from AD 1948–1998.⁴²
69x50mm (300 x 300 DPI)



20th Century trends in atmospheric Hg deposition at Mount Logan compared with ice core records of Pb pollution and the longest available measurements of remote atmospheric Hg concentrations. a) Mount Logan Hg_T fluxes (blue points) with 1 σ error bars and LOESS smoother (red line). Grey shading denotes two periods of elevated Hg_T fluxes. b) Annually averaged Pb concentrations in the Mount Logan ice core¹⁸ and the Eclipse Icefield ice core²⁸, both in the St. Elias Mountains, and in the Act2 ice core in southern Greenland²⁹. c) Modeled firn-air Hg⁰ concentrations in a core from Summit in central Greenland modified from Faïn et al.³⁰ d) Total filterable (particulate) Hg concentrations in air samples from Resolute in Arctic Canada modified from Li et al.³¹

68x111mm (300 x 300 DPI)



Multi-century Hg_T records from ice cores compared with estimates of primary anthropogenic emissions used in recent global Hg models. a) Mount Logan Hg_T fluxes (blue points) with 1σ error bars, LOESS smoother (red line), and inset with adjusted y-axis for the Preindustrial Period. b) Hg_T fluxes in the Upper Fremont Glacier ice core calculated using an assumed constant accumulation rate of 800 kg m⁻² a⁻¹ modified from Schuster et al.¹⁴ c) Estimated primary anthropogenic Hg emissions from industrial and mining sources modified from Streets et al.,⁷ and additional emissions from commercial Hg use modified from Horowitz et al.⁸

136x103mm (300 x 300 DPI)

An ice core perspective on mercury pollution during the past 600 years

Environmental Science and Technology

Samuel A. Beal^{*,1}, Erich C. Osterberg¹, Christian M. Zdanowicz², and David A. Fisher³

¹ Department of Earth Sciences, Dartmouth College, Hanover, New Hampshire, USA.

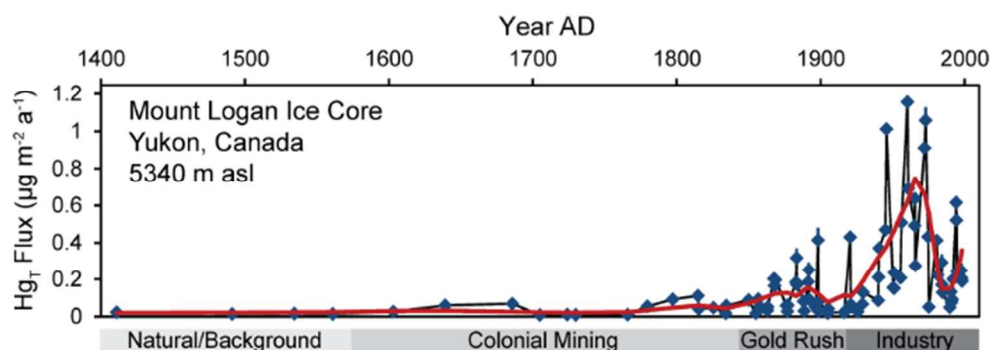
² Department of Earth Sciences, Uppsala University, Uppsala, Sweden.

³ Department of Earth Sciences, University of Ottawa, Ottawa, Ontario, Canada.

* Corresponding author: SA Beal; U.S. Army Corps of Engineers, Engineer Research and Development Center, Cold Regions Research and Engineering Laboratory; 72 Lyme Road, Hanover, NH 03755, United States; phone: 603-646-4125; email: samuel.beal@usace.army.mil

Keywords: mercury record; global mercury cycle; Mount Logan; metal pollution

TOC/Abstract Art



1 **Abstract (150-200 words)**

2 Past emissions of the toxic metal mercury (Hg) persist in the global environment, yet
3 these emissions remain poorly constrained by existing data. Ice cores are high-resolution
4 archives of atmospheric deposition that may provide crucial insight into past atmospheric Hg
5 levels during recent and historical time. Here we present a record of total Hg (Hg_T) in an ice core
6 from the pristine summit plateau (5340 m asl) of Mount Logan, Yukon, Canada, representing
7 atmospheric deposition from AD 1410 to 1998. The Colonial Period (~1603–1850) and North
8 American “Gold Rush” (1850–1900) represent minor fractions (8% and 14%, respectively) of
9 total anthropogenic Hg deposition in the record, with the majority (78%) occurring during the
10 20th Century. A period of maximum Hg_T fluxes from 1940 to 1975 coincides with estimates of
11 enhanced anthropogenic Hg emissions from commercial sources, as well as with industrial
12 emissions of other toxic metals. Rapid declines in Hg_T fluxes following peaks during the “Gold
13 Rush” and the mid-20th Century indicate that atmospheric Hg deposition responds quickly to
14 reductions in emissions. Increasing Hg_T fluxes from 1993 until the youngest samples in 1998
15 may reflect the resurgence of Hg emissions from unregulated coal burning and small-scale gold
16 mining.

17 **1. Introduction**

18 Atmospheric deposition of the globally distributed and toxic metal mercury (Hg)
19 contaminates ecosystems throughout the world.¹ Hg is introduced to the environment by *primary*
20 emissions from anthropogenic sources (e.g., coal burning, Hg mining, and silver and gold
21 mining) and natural sources (e.g., volcanism and weathering). Primary emissions occur
22 predominantly as gaseous Hg^0 , with lesser quantities of reactive Hg^{2+} species that are either

23 gaseous or bound to particulates (Hg_p).² With a residence time in the atmosphere of ~ 1 year, Hg^0
24 can be transported globally before oxidation to Hg^{2+} causes deposition to the land/ocean surface
25 in precipitation (wet deposition) or by particle settling (dry deposition).³ Deposited Hg can be
26 reemitted to the atmosphere through *secondary* emissions (e.g., ocean-air exchange and biomass
27 burning), which actively cycles Hg between the ocean, land, and atmosphere.^{4,5}

28 Recent works provide disparate accounts of past primary anthropogenic Hg emissions,
29 which are thought to have occurred since at least AD 1570.⁶ Framing this disparity are emissions
30 estimates, based on historical records of metal production and industrial/commercial activity, and
31 sediment records from remote lakes with small undisturbed watersheds. Emissions estimates
32 indicate that mining during the Preindustrial Period (pre-AD 1850) and the North American
33 “Gold Rush” (AD 1850–1920) represent $\sim 30\%$ and $\sim 27\%$, respectively, of total primary
34 anthropogenic Hg emissions, and that emission rates peaked in the 1970s.^{7,8} Conversely,
35 sediment records from remote lakes generally support background rates of atmospheric Hg
36 deposition ($\sim 1 \mu\text{g m}^{-2} \text{a}^{-1}$) until \sim AD 1850 and a subsequent continuous increase to the present-
37 day.⁹ Uncertainties in past emissions propagate to global model determinations of anthropogenic
38 Hg in the modern environment and predictions of the environmental response to future emissions
39 scenarios.

40 Ice cores are archives of atmospheric Hg deposition over seasonal to millennial
41 timescales, preserving a purely atmospheric signal with high temporal resolution and excellent
42 chronological control through annual layer counting and distinct event stratigraphy. Although an
43 unknown fraction of deposited Hg is reemitted to the atmosphere by photoreduction within the
44 upper 3 to 60 cm of snowpack,¹⁰ the remaining Hg that is preserved in glacial ice may reveal
45 important information on past changes in atmospheric Hg deposition. Records of total Hg (Hg_T)

46 from ice cores have been developed since the 1970s, but work in the 1990s by Boutron et al.
47 using clean methods for sample handling in the field and laboratory demonstrated that many of
48 these earlier records were contaminated by orders of magnitude.¹¹ Clean sampling of remote
49 glacial snow and ice typically reveals Hg_T concentrations from <0.02 to $\sim 4 \text{ pg g}^{-1}$.¹¹⁻¹³ To date,
50 the only published ice core Hg_T record covering the entire industrial period is from Upper
51 Fremont Glacier in Wyoming, United States.¹⁴ This record has been used extensively in literature
52 on the global Hg cycle,¹⁵ and it contains several unique characteristics including a prominent
53 “Gold Rush” peak, short-lived (2 to 3-year) peaks associated with explosive volcanic events in
54 both the Northern and Southern Hemisphere, and an abrupt decline in Hg_T concentrations in the
55 1980s.¹⁴ However, the unique characteristics of the record, relatively high Hg_T concentrations
56 ($1.2\text{--}35 \text{ pg g}^{-1}$), and the glacier’s proximity to upwind historical mining and industrial Hg
57 sources have led to uncertainty about the record’s representativeness of global trends in
58 atmospheric Hg.^{9,15} New ice core Hg_T records from remote glaciers could provide useful
59 additional constraints on past global Hg emissions.

60 Here we present a record of Hg_T from AD 1410 to 1998 in an ice core from Mount
61 Logan, Yukon, Canada. The Mount Logan ice core, collected from the mountain’s summit
62 plateau (5340 m asl), preserves deposition from the free troposphere sourced by winds traversing
63 the North Pacific Ocean (Figure 1).^{16,17} The core’s location, tightly constrained chronology, and
64 high-resolution co-registered geochemistry¹⁸ allow us to interpret the Mount Logan Hg_T record
65 and assess its relevance to past global Hg emissions.

66 2. Materials and Methods

67 2.1. Core Collection

68 The Mount Logan ice core was collected from Prospector-Russell Col on the summit
69 plateau (5340 m asl) of Mount Logan in the summers of 2001 and 2002 by the Geological
70 Survey of Canada. The coring site is near the center of dividing glacier flow with low ice
71 velocities ($<0.2 \text{ m a}^{-1}$), and the site has persistent below-freezing temperatures based on
72 automatic weather station data (mean annual: -29°C) and the lack of refrozen surface melt layers
73 in the core.^{19,20} The core was collected from a dry borehole using an electromechanical drill from
74 2 m depth until bedrock at 186 m depth. We focus on the depth range of 3 to 128 m that
75 represents net snow accumulation between AD 1410 and 1998. Previous work established the
76 depth-age model for this ice core based on annual layer counting of seasonal oscillations in $\delta^{18}\text{O}$
77 and Na and U concentrations between 1700 and 1998 (3–109 m depth) and an ice flow model
78 constrained by well-dated volcanic signals between 1410 and 1700 (109–128 m depth).^{18,21,22}

79 2.2. Core Decontamination

80 We sampled discrete sections of the ice core, with each section comprising at least one
81 complete year of accumulation. Within the upper 100 m of the ice core, which included firn (3–
82 45 m depth) and ice (45–100 m depth), the volume of material for each section required division
83 into multiple samples that we plot individually. We melted firn and ice samples in 500-ml glass
84 jars with PTFE septa and polypropylene caps which we pre-cleaned following Method B in
85 Hammerschmidt et al.²³ Briefly, this cleaning method involved successive storage in a Citranox
86 and $>18.2 \text{ M}\Omega$ deionized (DI) water solution for 6 days, in 10% Trace-Metal Grade HCl for 6
87 days, and in 1% BrCl (made from reagent grade KBr, KBrO_3 , and Optima HCl) for 1 day. All
88 sample work was conducted in a HEPA-filtered laminar flow bench with a double layer of

89 activated carbon cloth covering the filter air intake. We cut firm and ice pieces that were longer
90 than 10 cm with a stainless steel saw to accommodate the height of the glass jars. For firm
91 samples (3–45 m), we manually removed the outer surfaces of each sample using ZrO ceramic
92 knives (pre-cleaned with 10% HCl) in a -10 °C freezer before transferring the decontaminated
93 firm to the pre-cleaned glass jars. For ice samples (45–128 m), we removed potentially
94 contaminated outer ice surfaces by partially melting each sample for 1.5 hours at room
95 temperature in Whirlpak bags before rinsing with DI water and transferring to the pre-cleaned
96 glass jars. We tested contamination of outer ice core surfaces by partially melting selected ice
97 samples in pre-cleaned glass jars instead of Whirlpak bags, and then treating the cleanly
98 collected meltwater from the outer core surfaces as samples. We made procedural blanks by
99 freezing low-Hg ($<0.02 \text{ pg g}^{-1}$) DI water in pre-cleaned glass jars and processed them following
100 the decontamination methods for either firm or ice. Before melting, we added concentrated BrCl
101 to each sample or procedural blank to a final concentration of 0.1% BrCl.²⁴

102 **2.3. Hg_T Analysis**

103 Within 72 hours of melting, we measured Hg_T in ~24 ml sample aliquots using Purge and
104 Trap with Cold Vapor Atomic Fluorescence Spectrometry (Brooks Rand Automated Total
105 Mercury Analyzer) following EPA Method 1631E. Hg_T refers to all BrCl-oxidizable forms of Hg
106 present, including Hg²⁺, Hg⁰, organic Hg, and Hg adsorbed to particulates.²⁴ The instrumental
107 detection limit was 0.02 pg g^{-1} , but the method detection limit (MDL; determined here as 3σ of
108 the procedural blanks) ranged from 0.01 to 0.24 pg g^{-1} (median 0.06) depending on the method
109 and day of sampling. Sample concentrations were considered detectable if their procedural blank
110 subtracted concentrations exceeded the MDL.

111 2.4. Flux Calculations

112 We determine Hg_T fluxes as the product of measured Hg_T concentrations and water
113 equivalent accumulation rates (ARs). In the Mount Logan ice core, ARs are calculated within the
114 sub-annually resolved portion of the core (1700–1998) from measurements of density (kg m^{-3})
115 and annual layer thickness (m a^{-1}), and ARs are estimated within the annually resolved portion of
116 the core (1410–1700) as the average of measured ARs from the sub-annually resolved portion
117 ($420 \pm 90 \text{ kg m}^{-2} \text{ a}^{-1}$) because annual layer thickness is not accurately determined at these
118 depths.¹⁸

119 3. Results and Discussion

120 Of the 130 samples that we melted, 88 samples had detectable Hg_T concentrations (Table
121 1 and Figure S1). Table 1 shows the occasionally high and variable procedural blank values that
122 limited detection of Hg_T in the remaining samples. We suspect that day-to-day changes in air
123 quality within the HEPA-filtered laminar flow benches are responsible for this variability,
124 highlighting the need for the many procedural blanks used in this study. Among the samples with
125 detectable Hg_T concentrations, preservation of a signal from atmospheric Hg deposition is
126 supported by similar Hg_T concentrations found in snow/ice from other remote glaciers^{11–13} and
127 by the order of magnitude concentration difference between the samples and the core exterior
128 removed during decontamination (Table 1).

129 In the most recent samples from 1994 to 1998, Hg_T fluxes ($0.19\text{--}0.52 \text{ } \mu\text{g m}^{-2} \text{ a}^{-1}$) are an
130 order of magnitude lower than recent measurements of wet deposition across the western United
131 States ($\sim 1\text{--}9 \text{ } \mu\text{g m}^{-2} \text{ a}^{-1}$) and in sub-Arctic Alaska and Canada ($\sim 1\text{--}5 \text{ } \mu\text{g m}^{-2} \text{ a}^{-1}$).^{25,26} This
132 difference could be attributed to the relative inefficiency of gaseous Hg^{2+} scavenging by snow,²⁷
133 which is the only phase of precipitation at Mount Logan, and to the reemission of a fraction of

134 deposited Hg from the snowpack. Repeated sampling of surface snows generally indicate that
135 >50% of Hg is reemitted within 24 hours, although there is great variability both within
136 individual study sites and between geographic areas.¹⁰ Nevertheless, we propose that multi-
137 annual variations in the Mount Logan Hg_T flux record reflect past changes in mid-tropospheric
138 atmospheric Hg²⁺ deposition based on several lines of evidence. First, the estimated Hg⁰ content
139 in firn/ice air can account for only 0.2 to 7% of the measured Hg_T concentrations (see Supporting
140 Information). Hg_T concentrations are only weakly correlated with co-registered lithogenic
141 element and Pb concentrations ($r = 0.23\text{--}0.35$, $p < 0.05$), which are proxies for Hg_p from crustal
142 and industrial sources, respectively (Table S1). Hg_T concentrations are neither correlated with
143 co-registered chloride concentrations, nor with ARs (Table S1), both of which are thought to
144 affect Hg reemission from the snowpack.^{10,28} Finally, the Mount Logan Hg_T flux record shows
145 striking similarities with two of the longest published records of remote atmospheric Hg levels
146 (Figure 2) and with historical changes in Hg use, which we discuss below. On shorter (sub-
147 annual to annual) timescales, the relatively high variability, or spikiness, of the Mount Logan
148 Hg_T flux record is likely the result of factors influencing Hg reemission from the snowpack.
149 Accordingly, we use a LOESS smoothed line to filter out this short-term variability and highlight
150 longer-term variations in the Mount Logan Hg_T flux record.

151 **3.1. The 20th Century**

152 Figure 2 shows the Mount Logan Hg_T record during the 20th Century, revealing near-
153 background Hg_T fluxes ($0.02\text{--}0.06 \mu\text{g m}^{-2} \text{a}^{-1}$) from 1900 to 1940, a broad peak between ~1940
154 and 1975 (maximum of $1.2 \mu\text{g m}^{-2} \text{a}^{-1}$ in 1960), decreasing fluxes during the 1980s, and a final
155 rise through the 1990s. Comparison with high resolution Pb records from the Mount Logan ice
156 core and other high northern latitude glaciers provide information on both the source and

157 speciation of Hg_T in the Mount Logan ice core. The mid-century peak in Mount Logan Hg_T
158 fluxes is coincident with a period of maximum Pb deposition registered in ice cores from
159 Greenland and from Eclipse Icefield (located ~50 km northwest of Mount Logan at 3017 m asl),
160 attributed to industrial (e.g., coal burning) aerosol emissions from North America and Europe
161 that increased from World War II until the enactment of environmental regulations in the 1970s
162 (Figure 2b).^{29,30} However, North American and European Pb aerosols did not reach the Mount
163 Logan summit plateau during this time (Figure 2b) because of the relatively short (7-10 days)
164 atmospheric residence time of Pb,³¹ and the persistent air mass source from the west (North
165 Pacific and Asia) due to the site's elevation in the free troposphere.¹⁸ Different emissions sources
166 for 20th Century Pb and Hg deposited on Mount Logan is also supported by the lack of
167 correlation between the two co-registered records (Table S1). Rather, the mid-century peak in
168 Mount Logan Hg_T fluxes mirrors a record of atmospheric Hg^0 concentrations from firn-air at
169 Summit Greenland (Figure 2c). Altogether, these comparisons suggest a coherent change in high
170 northern latitude atmospheric Hg levels during the 20th Century associated with industrial
171 emissions from North America and Europe.

172 Subsequent to the mid-century peak, Hg_T fluxes decline during the 1980s and approach
173 near-background fluxes ($0.05\text{--}0.13 \mu\text{g m}^{-2} \text{a}^{-1}$) between 1989 and 1991. Decreases during this
174 time are similarly observed in the firn-air Hg^0 record from Summit Greenland³² and in air
175 measurements of Hg_p at Resolute Bay in the Canadian High Arctic (Figure 2d).³³ A record-
176 maximum peak in Mount Logan Pb concentrations between 1980 and 1989, likely resulting from
177 the transport and deposition of industrial aerosols from Asia,¹⁸ is coincident with this period of
178 depressed Mount Logan Hg_T fluxes and therefore indicative of negligible Hg_p contributions from
179 Asia during this time. We sampled the Mount Logan ice core at continuous 0.5-year resolution

180 between late 1989 and late 1991 to examine a possible Hg_T pulse from the April 2, 1991 eruption
181 of Mount Pinatubo that sent volcanic ash and sulfur-containing aerosols into the stratosphere.³⁴
182 Such a pulse is not evident in either the Mount Logan or the Upper Fremont Glacier records
183 during the timing of this eruption.¹⁴ A number of other major volcanic eruptions, including ones
184 in the Southern Hemisphere, are identified as significant Hg_T spikes, in the Upper Fremont
185 Glacier record,¹⁴ but material from the Mount Logan ice core covering these events has been
186 entirely consumed for other studies.

187 Increasing Mount Logan Hg_T fluxes from 1993 until 1998 (the age of the youngest
188 samples) coincide with estimated increasing emissions of Hg^0 , Hg_p , and Pb from coal
189 combustion in Asia.^{7,35} The trans-Pacific transport and deposition of industrial aerosols from
190 Asia are thought to be responsible for increasing Pb concentrations in the Mount Logan ice core
191 during the 1990s (Figure 2b).¹⁸ We therefore infer that the increase in Hg_T fluxes between 1993
192 and 1998 is due, at least in part, to deposition of Hg_p associated with Asian industrial emissions.

193 **3.2. The “Gold Rush” (AD 1850–1900)**

194 Figure 3 displays the entire 600-year Mount Logan record, which shows, in addition to
195 the mid-20th Century peak, a smaller irregular peak in Hg_T fluxes that begins in the 1860s,
196 reaches a maximum of $0.32 \mu\text{g m}^{-2} \text{a}^{-1}$ in ~1883, and remains elevated until a return to
197 background at the turn of the century. This 19th Century peak is largely synchronous with an
198 estimated peak in primary Hg emissions from silver and gold mining in North America, and
199 associated Hg production (mainly in Spain, Slovenia, and Italy), during the “Gold Rush”
200 between 1860 and 1920 (Figure 3c).⁷ The Upper Fremont Glacier Hg_T record (Figure 3b) also
201 shows a “Gold Rush” peak, which the authors suggest is caused by the regional transport and
202 deposition of Hg from gold mining in upwind California.¹⁴ The synchronous response of the

203 Mount Logan Hg_T flux record to estimated global Hg emissions during the “Gold Rush”, and the
204 lack of major upwind Hg point sources during the time, support a distinct anthropogenic change
205 in high northern latitude Hg levels caused by the “Gold Rush”. However, the Mount Logan and
206 Upper Fremont Glacier “Gold Rush” Hg_T peaks are both substantially smaller than their
207 respective 20th Century peaks, whereas emissions estimates indicate that the “Gold Rush”
208 included an extended period of some of the highest primary anthropogenic Hg emissions of the
209 past 400 years (Figure 3).^{7,8} Lower-than-estimated anthropogenic Hg emissions during the “Gold
210 Rush” may explain the lack of such a signal in many lake sediment records.⁹

211 3.3. The Preindustrial Period (AD 1410–1850)

212 The inset of Figure 3a shows stable background Mount Logan Hg_T fluxes (0.015–0.023
213 $\mu\text{g m}^{-2} \text{a}^{-1}$) from ~1410 to ~1561, followed by a period of increased low-level variability in Hg_T
214 fluxes lasting until ~1850, when the impact of industrial emissions becomes clearly apparent.
215 The introduction in 1570 of liquid Hg^0 for silver mining in Colonial Spanish South America
216 likely marked the first global distribution of anthropogenic Hg,^{6,36,37} so we interpret the Mount
217 Logan Hg_T fluxes prior to 1570 as representative of natural deposition and subsequent variations
218 from this background as due to anthropogenic Hg emissions. The background pre-Colonial Hg_T
219 fluxes are in good agreement with a few measurements of Hg_T ($0.009 \mu\text{g m}^{-2} \text{a}^{-1}$) during the early
220 and middle Holocene in an ice core from Dome C, Antarctica.³⁸ The low-level increases in
221 Mount Logan Hg_T fluxes between ~1600 and 1850 suggest that Hg emissions from Colonial
222 silver mining were globally transported, however Hg_T fluxes during this time are at least an order
223 of magnitude lower than Hg_T fluxes during both the “Gold Rush” and the late 20th Century.

224 3.4. Potential Global Hg Cycle Implications

225 Integrating the smoothed Mount Logan Hg_T flux record (Figure 3a) after subtracting
226 average background (1410–1561) fluxes yields ~78% of anthropogenic Hg deposition registered
227 by the ice core occurring during the 20th Century, ~14% during the “Gold Rush” (1850–1900),
228 and ~8% during the Colonial Period (~1603–1850). This 20th Century dominance in the Mount
229 Logan record differs significantly from estimates of primary anthropogenic Hg emissions from
230 industrial, mining, and commercial sources, which combined show that the “Gold Rush” and
231 Preindustrial Period contributed ~27% and ~30% of total anthropogenic emissions,
232 respectively.^{7,8} Hg releases to water and soil may emit additional anthropogenic Hg to the
233 atmosphere, but estimates of these releases generally scale with total (commercial, industrial, and
234 mining) primary emissions since 1850.⁸ The potential for secondary emissions from the oceans
235 and land to influence deposition across the time periods discussed here make this a first-order
236 comparison. However, the relatively small anthropogenic Hg deposition registered by the Mount
237 Logan ice core before 1900 suggests that current estimates of Hg emissions from Colonial and
238 “Gold Rush” mining are erroneously high. In turn, global Hg models forced with these high
239 emissions likely overestimate the influence of early mining on anthropogenic Hg in the modern
240 global environment.

241 Rapid declines in the Hg_T flux records from both Mount Logan and Upper Fremont
242 Glacier coincide with estimated decreases in primary anthropogenic emissions from mining
243 following the “Gold Rush”⁷ and from commercial sources in the 1970s⁸ (Figure 3). However,
244 global Hg models forced with these emissions estimates show relatively minor decreases in
245 atmospheric Hg following the “Gold Rush” and the 1970s, which are the result of high emission
246 forcings from early mining and secondary emissions that are estimated as approximately

247 equivalent to primary emissions during the present-day.^{4,5,8,39} Similar to the ice core Hg_T records,
248 the Summit Greenland firn-air Hg^0 record (Figure 2c) exhibits a rapid decrease following the
249 1970s, but the extent of its recovery is difficult to assess because of the record's brevity and the
250 potential for smoothing by diffusion of gaseous Hg^0 .³² The rapid decreases in atmospheric Hg
251 deposition implied by the Mount Logan and Upper Fremont Glacier records may not be easily
252 detectable in lake sediment records due to lagged declines in watershed inputs.⁴⁰ However,
253 decreases following both the "Gold Rush" and the 1970s are apparent in Hg flux records from
254 two remote lakes with exceptional characteristics: the crater lake Challa in eastern equatorial
255 Africa (900 m asl) that has almost no surficial watershed,⁹ and the tarn Yanacocha in southern
256 Peru (4900 m asl) that has a small, poorly vegetated watershed composed predominantly of
257 exposed bedrock.⁴¹ Further research is needed to constrain net exchanges between the land,
258 oceans, and atmosphere that cause anthropogenic Hg to persist in the environment.

259 Rising Hg_T fluxes during the most recent part of the Mount Logan record, from 1993 to
260 1998, may reflect a new period of increasing primary Hg emissions, driven by coal burning in
261 Asia and small-scale gold mining in developing countries around the world, that is estimated to
262 have continued at least through 2008.^{2,7} Remarkably, however, the majority of atmospheric
263 measurements, primarily from the Atlantic near sea level, reveal declining Hg^0 concentrations
264 from ~2000 to 2009.^{42,43} New high-resolution records of atmospheric Hg deposition, in addition
265 to air measurements, are needed to document trends in global atmospheric Hg pollution and to
266 address fundamental deficiencies in our current understanding of the global Hg cycle. The
267 collection of new ice cores for this work demands urgency as glaciers around the world are
268 currently experiencing accelerated mass losses, and many may soon vanish.^{44,45}

269 Acknowledgments

270 This material is based upon work supported by the National Science Foundation under Grant No.
271 BCS-1232844. We thank the following collaborators: the Geological Survey of Canada for
272 making the Mount Logan ice core available; T. Overly and G. Wong for ice core processing in
273 Ottawa; Z. Courville for freezer access; B. Jackson and C. Lamborg for scientific insight; and J.
274 Creswell and V. Engel at Brooks Rand Labs for instrument assistance. We also thank four
275 anonymous reviewers.

276 Supporting Information Available

277 The primary data for this paper can be accessed in the Supporting Information. This information
278 is available free of charge via the Internet at <http://pubs.acs.org>.

279 References

- 280 (1) Fitzgerald, W. F.; Engstrom, D. R.; Mason, R. P.; Nater, E. A. The Case for Atmospheric
281 Mercury Contamination in Remote Areas. *Environ. Sci. Technol.* **1998**, *32* (1), 1–7.
- 282 (2) Pacyna, E. G.; Pacyna, J. M. Global Emission of Mercury from Anthropogenic Sources in
283 1995. *Water Air Soil Poll* **2002**, *137* (1), 149–165.
- 284 (3) Lamborg, C. H.; Fitzgerald, W. F.; Damman, A. W. H.; Benoit, J. M.; Balcom, P. H.;
285 Engstrom, D. R. Modern and historic atmospheric mercury fluxes in both hemispheres:
286 Global and regional mercury cycling implications. *Global Biogeochem. Cycles* **2002**, *16*
287 (4), 51–1 – 51–11.
- 288 (4) Friedli, H. R.; Arellano, A. F.; Cinnirella, S.; Pirrone, N. Initial Estimates of Mercury
289 Emissions to the Atmosphere from Global Biomass Burning. *Environ. Sci. Technol.* **2009**,
290 *43* (10), 3507–3513.
- 291 (5) Soerensen, A. L.; Sunderland, E. M.; Holmes, C. D.; Jacob, D. J.; Yantosca, R. M.; Skov,
292 H.; Christensen, J. H.; Strode, S. A.; Mason, R. P. An Improved Global Model for Air-Sea
293 Exchange of Mercury: High Concentrations over the North Atlantic. *Environ. Sci.*
294 *Technol.* **2010**, *44* (22), 8574–8580.
- 295 (6) Nriagu, J. O. Legacy of mercury pollution. *Nature* **1993**, *363* (6430), 589–589.
- 296 (7) Streets, D. G.; Devane, M. K.; Lu, Z.; Bond, T. C.; Sunderland, E. M.; Jacob, D. J. All-
297 Time Releases of Mercury to the Atmosphere from Human Activities. *Environ Sci*
298 *Technol* **2011**, *45* (24), 10485–10491.
- 299 (8) Horowitz, H. M.; Jacob, D. J.; Amos, H. M.; Streets, D. G.; Sunderland, E. M. Historical
300 Mercury Releases from Commercial Products: Global Environmental Implications.
301 *Environ. Sci. Technol.* **2014**, *48* (17), 10242–10250.

- 302 (9) Engstrom, D. R.; Fitzgerald, W. F.; Cooke, C. A.; Lamborg, C. H.; Drevnick, P. E.;
303 Swain, E. B.; Balogh, S. J.; Balcom, P. H. Atmospheric Hg emissions from preindustrial
304 gold and silver extraction in the Americas: a reevaluation from lake-sediment archives.
305 *Environ Sci Technol* **2014**, *48* (12), 6533–6543.
- 306 (10) Durnford, D.; Dastoor, A. The behavior of mercury in the cryosphere: A review of what
307 we know from observations. *J Geophys Res* **2011**, *116*, D06305.
- 308 (11) Boutron, C. F.; Vandal, G. M.; Fitzgerald, W. F.; Ferrari, C. P. A forty year record of
309 Mercury in central Greenland snow. *Geophys Res Lett* **1998**, *25* (17), 3315–3318.
- 310 (12) Zdanowicz, C.; Krümmel, E. M.; Lean, D.; Poulain, A. J.; Yumvihoze, E.; Chen, J.;
311 Hintelmann, H. Accumulation, storage and release of atmospheric mercury in a glaciated
312 Arctic catchment, Baffin Island, Canada. *Geochim Cosmochim Acta* **2013**, *107* (0), 316–
313 335.
- 314 (13) Zheng, J.; Pelchat, P.; Vaive, J.; Bass, D.; Ke, F. Total mercury in snow and ice samples
315 from Canadian High Arctic ice caps and glaciers: A practical procedure and method for
316 total Hg quantification at low pg g⁻¹ level. *Sci Total Environ* **2014**, *468–469* (0), 487–
317 494.
- 318 (14) Schuster, P. F.; Krabbenhoft, D. P.; Naftz, D. L.; Cecil, L. D.; Olson, M. L.; Dewild, J. F.;
319 Susong, D. D.; Green, J. R.; Abbott, M. L. Atmospheric Mercury Deposition during the
320 Last 270 Years: A Glacial Ice Core Record of Natural and Anthropogenic Sources.
321 *Environ Sci Technol* **2002**, *36* (11), 2303–2310.
- 322 (15) UNEP. *Global Mercury Assessment 2013: Sources, Emissions, Releases and*
323 *Environmental Transport*; DTI/1636/GE; UNEP Chemicals Branch: Geneva, Switzerland,
324 2013.
- 325 (16) Zdanowicz, C.; Hall, G.; Vaive, J.; Amelin, Y.; Percival, J.; Girard, I.; Biscaye, P.; Bory,
326 A. Asian dustfall in the St. Elias Mountains, Yukon, Canada. *Geochim Cosmochim Acta*
327 **2006**, *70* (14), 3493–3507.
- 328 (17) Zdanowicz, C.; Fisher, D.; Bourgeois, J.; Demuth, M.; Zheng, J.; Mayewski, P.; Kreutz,
329 K.; Osterberg, E.; Yalcin, K.; Wake, C.; et al. Ice Cores from the St. Elias Mountains,
330 Yukon, Canada: Their Significance for Climate, Atmospheric Composition and Volcanism
331 in the North Pacific Region. *ARCTIC; Vol 67, No 5 (2014): Supplement 1: 1–107* **2014**.
- 332 (18) Osterberg, E.; Mayewski, P.; Kreutz, K.; Fisher, D.; Handley, M.; Sneed, S.; Zdanowicz,
333 C.; Zheng, J.; Demuth, M.; Waskiewicz, M.; et al. Ice core record of rising lead pollution
334 in the North Pacific atmosphere. *Geophys Res Lett* **2008**, *35* (5), L05810.
- 335 (19) Fisher, D. A.; Wake, C.; Kreutz, K.; Yalcin, K.; Steig, E.; Mayewski, P.; Anderson, L.;
336 Zheng, J.; Rupper, S.; Zdanowicz, C.; et al. Stable Isotope Records from Mount Logan,
337 Eclipse Ice Cores and Nearby Jellybean Lake. Water Cycle of the North Pacific Over 2000
338 Years and Over Five Vertical Kilometers: Sudden Shifts and Tropical Connections.
339 *Geogr. Phys. Quat.* **2004**, *58* (2-3), 337–352.
- 340 (20) Holdsworth, G.; Krouse, H. R.; Nosal, M. Ice core climate signals from Mount Logan,
341 Yukon A.D. 1700-1897. In *Climate Since AD 1500*; Routledge: London and New York,
342 1992; pp 483–504.
- 343 (21) Fisher, D.; Osterberg, E.; Dyke, A.; Dahl-Jensen, D.; Demuth, M.; Zdanowicz, C.;
344 Bourgeois, J.; Koerner, R. M.; Mayewski, P.; Wake, C.; et al. The Mt Logan Holocene—
345 late Wisconsinan isotope record: tropical Pacific—Yukon connections. *The Holocene*
346 **2008**, *18* (5), 667–677.

- 347 (22) Fisher, D. Connecting the Atlantic-sector and the north Pacific (Mt Logan) ice core stable
348 isotope records during the Holocene: The role of El Niño. *The Holocene* **2011**, *21* (7),
349 1117.
- 350 (23) Hammerschmidt, C. R.; Bowman, K. L.; Tabatchnick, M. D.; Lamborg, C. H. Storage
351 bottle material and cleaning for determination of total mercury in seawater. *Limnol*
352 *Oceanogr-Meth* **2011**, *9*, 426–431.
- 353 (24) EPA. Method 1631, Revision E: Mercury in Water by Oxidation, Purge and Trap, and
354 Cold Vapor Atomic Fluorescence Spectrometry, 2002.
- 355 (25) NADP. *National Atmospheric Deposition Program (NRSP-3)*; NADP Program Office
356 Illinois State Water Survey: 2204 Griffith Dr., Champaign, IL 61820, 2007.
- 357 (26) Sanei, H.; Outridge, P. M.; Goodarzi, F.; Wang, F.; Armstrong, D.; Warren, K.; Fishback,
358 L. Wet deposition mercury fluxes in the Canadian sub-Arctic and southern Alberta,
359 measured using an automated precipitation collector adapted to cold regions. *Atmospheric*
360 *Environment* **2010**, *44* (13), 1672–1681.
- 361 (27) Mao, H.; Talbot, R.; Hegarty, J.; Koermer, J. Speciated mercury at marine, coastal, and
362 inland sites in New England – Part 2: Relationships with atmospheric physical parameters.
363 *Atmospheric Chemistry and Physics* **2012**, *12* (9), 4181–4206.
- 364 (28) Lalonde, J. D.; Amyot, M.; Doyon, M.-R.; Auclair, J.-C. Photo-induced Hg(II) reduction
365 in snow from the remote and temperate Experimental Lakes Area (Ontario, Canada). *J.*
366 *Geophys. Res.* **2003**, *108* (D6), 4200.
- 367 (29) Gross, B. H.; Kreutz, K. J.; Osterberg, E. C.; McConnell, J. R.; Handley, M.; Wake, C. P.;
368 Yalcin, K. Constraining recent lead pollution sources in the North Pacific using ice core
369 stable lead isotopes. *J Geophys Res-Atmos* **2012**, *117*, D16307–D16307.
- 370 (30) McConnell, J. R.; Edwards, R. Coal burning leaves toxic heavy metal legacy in the Arctic.
371 *Proc Natl Acad Sci USA* **2008**, *105* (34), 12140–12144.
- 372 (31) Pilgrim, W.; Hughes, R. Lead, cadmium, arsenic and zinc in the ecosystem surrounding a
373 lead smelter. *Environ Monit Assess* **1994**, *32* (1), 1–20.
- 374 (32) Faïn, X.; Ferrari, C. P.; Dommergue, A.; Albert, M. R.; Battle, M.; Severinghaus, J.;
375 Arnaud, L.; Barnola, J.-M.; Cairns, W.; Barbante, C.; et al. Polar firn air reveals large-
376 scale impact of anthropogenic mercury emissions during the 1970s. *Proc Natl Acad Sci*
377 *USA* **2009**, *106* (38), 16114–16119.
- 378 (33) Li, C.; Cornett, J.; Willie, S.; Lam, J. Mercury in Arctic air: The long-term trend. *Sci Total*
379 *Environ* **2009**, *407* (8), 2756–2759.
- 380 (34) Siebert, L.; Simkin, S. *Volcanoes of the world: An illustrated catalogue of Holocene*
381 *volcanoes and their eruptions*. Smithsonian Institution, Global Volcanism Program Digital
382 Information Series, GVP-3. **2002**.
- 383 (35) Pacyna, J. M.; Pacyna, E. G. An assessment of global and regional emissions of trace
384 metals to the atmosphere from anthropogenic sources worldwide. *Environ Rev* **2001**, *9* (4),
385 269.
- 386 (36) Cooke, C. A.; Balcom, P. H.; Biester, H.; Wolfe, A. P. Over three millennia of mercury
387 pollution in the Peruvian Andes. *Proc Natl Acad Sci USA* **2009**, *106* (22), 8830–8834.
- 388 (37) Beal, S. A.; Kelly, M. A.; Stroup, J. S.; Jackson, B. P.; Lowell, T. V.; Tapia, P. M. Natural
389 and anthropogenic variations in atmospheric mercury deposition during the Holocene near
390 Quelccaya Ice Cap, Peru. *Global Biogeochem Cy* **2014**, *28*, 437–450.
- 391 (38) Vandal, G. M.; Fitzgerald, W. F.; Boutron, C. F.; Candelone, J.-P. Variations in mercury
392 deposition to Antarctica over the past 34,000 years. *Nature* **1993**, *362* (6421), 621–623.

- 393 (39) Amos, H. M.; Jacob, D. J.; Streets, D. G.; Sunderland, E. M. Legacy impacts of all-time
394 anthropogenic emissions on the global mercury cycle. *Global Biogeochem Cy* **2013**, *27*
395 (2), 410–421.
- 396 (40) Harris, R. C.; Rudd, J. W. M.; Amyot, M.; Babiarz, C. L.; Beaty, K. G.; Blanchfield, P. J.;
397 Bodaly, R. A.; Branfireun, B. A.; Gilmour, C. C.; Graydon, J. A.; et al. Whole-ecosystem
398 study shows rapid fish-mercury response to changes in mercury deposition. *Proc Natl*
399 *Acad Sci USA* **2007**, *104* (42), 16586–16591.
- 400 (41) Beal, S. A.; Jackson, B. P.; Kelly, M. A.; Stroup, J. S.; Landis, J. D. Effects of historical
401 and modern mining on mercury deposition in southeastern Peru. *Environ. Sci. Technol.*
402 **2013**, *47* (22), 12715–12720.
- 403 (42) Slemr, F.; Brunke, E.-G.; Ebinghaus, R.; Kuss, J. Worldwide trend of atmospheric
404 mercury since 1995. *Atmospheric Chemistry and Physics* **2011**, *11* (10), 4779–4787.
- 405 (43) Cole, A. S.; Steffen, A.; Pfaffhuber, K. A.; Berg, T.; Pilote, M.; Poissant, L.; Tordon, R.;
406 Hung, H. Ten-year trends of atmospheric mercury in the high Arctic compared to
407 Canadian sub-Arctic and mid-latitude sites. *Atmos. Chem. Phys.* **2013**, *13* (3), 1535–1545.
- 408 (44) Clarke, G. K. C.; Jarosch, A. H.; Anslow, F. S.; Radic, V.; Menounos, B. Projected
409 deglaciation of western Canada in the twenty-first century. *Nature Geosci* **2015**, *8* (5),
410 372–377.
- 411 (45) Lenaerts, J. T. M.; van Angelen, J. H.; van den Broeke, M. R.; Gardner, A. S.; Wouters,
412 B.; van Meijgaard, E. Irreversible mass loss of Canadian Arctic Archipelago glaciers.
413 *Geophys. Res. Lett.* **2013**, *40* (5), 870–874.
- 414 (46) Kalnay, E. The NCEP/NCAR Reanalysis 40-year Project. *B Am Meteorol Soc* **1996**, *77*,
415 437–471.

416 Tables

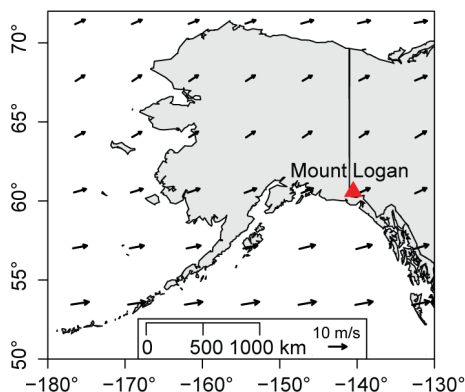
417 **Table 1.** Descriptive statistics for detectable Hg_T concentrations in samples, procedural blanks, and outer
418 core material removed during decontamination of Mount Logan firn and ice. Concentrations for samples
419 and the outer core are procedural blank corrected, whereas procedural blank concentrations are
420 instrumental blank (0.02 pg g⁻¹) corrected.

	Hg _T (pg g ⁻¹)				
	Firn		Ice		
	Samples	Proc. Blank	Samples	Proc. Blank	Outer Core
Max	3.52	0.33	1.06	0.34	9.41
Min	0.13	0.16	0.02	0.01	0.35
Mean	0.91	0.24	0.21	0.09	5.63
Median	0.66	0.23	0.14	0.04	5.41
Std. dev	0.82	0.06	0.23	0.10	2.29
n	37	12	51	43	13

421

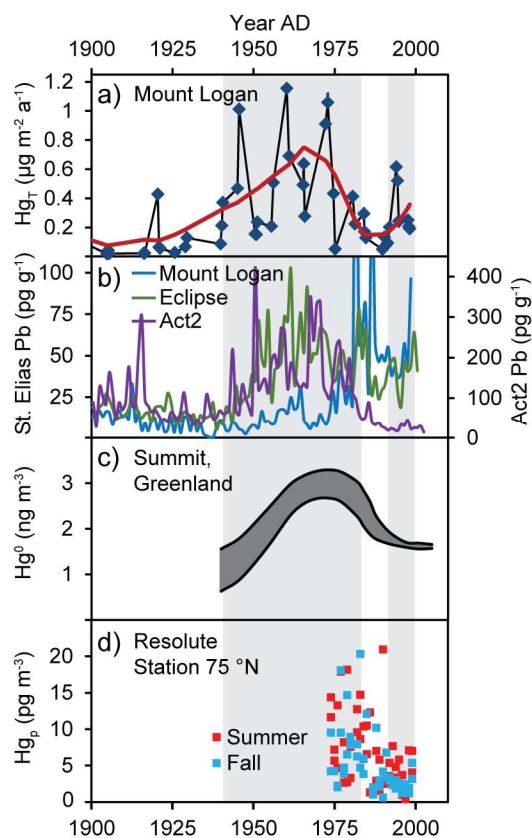
422 **Figures**

423



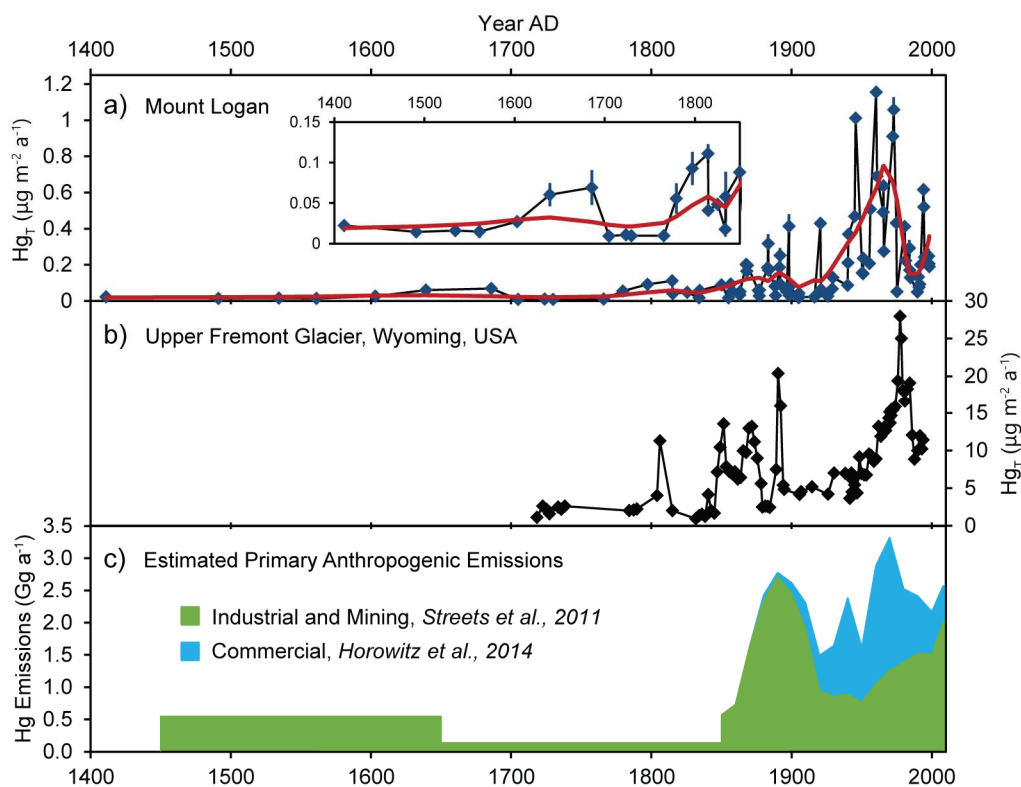
424 **Figure 1.** Location of Mount Logan (red triangle) in the St. Elias Mountains on the border of Alaska and
 425 Yukon, Canada. Arrows represent annual average vector wind at 500 mb from AD 1948–1998.⁴⁶

426

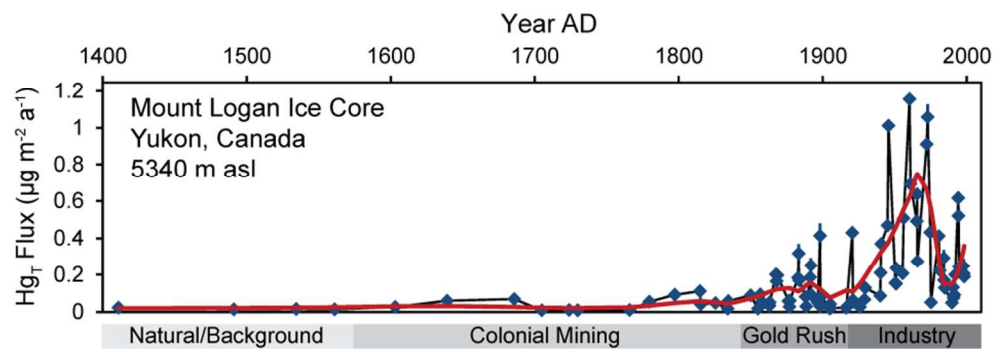


427 **Figure 2.** 20th Century trends in atmospheric Hg deposition at Mount Logan compared with ice core
 428 records of Pb pollution and the longest available measurements of remote atmospheric Hg concentrations.
 429 a) Mount Logan Hg_T fluxes (blue points) with 1σ error bars and LOESS smoother (red line). Grey
 430 shading denotes two periods of elevated Hg_T fluxes. b) Annually averaged Pb concentrations in the Mount
 431 Logan ice core¹⁸ and the Eclipse Icefield ice core,²⁹ both in the St. Elias Mountains, and in the Act2 ice
 432 core in southern Greenland.³⁰ c) Modeled firn-air Hg⁰ concentrations in a core from Summit in central

433 Greenland modified from Faïn et al.³² d) Total filterable (particulate) Hg concentrations in air samples
 434 from Resolute in Arctic Canada modified from Li et al.³³



435
 436 **Figure 3.** Multi-century Hg_T records from ice cores compared with estimates of primary anthropogenic
 437 emissions used in recent global Hg models. a) Mount Logan Hg_T fluxes (blue points) with 1σ error bars,
 438 LOESS smoother (red line), and inset with adjusted y-axis for the Preindustrial Period. b) Hg_T fluxes in
 439 the Upper Fremont Glacier ice core calculated using an assumed constant accumulation rate of 800 kg m⁻²
 440 a⁻¹ modified from Schuster et al.¹⁴ c) Estimated primary anthropogenic Hg emissions from industrial and
 441 mining sources modified from Streets et al.,⁷ and additional emissions from commercial Hg use modified
 442 from Horowitz et al.⁸



82x29mm (300 x 300 DPI)